

EVALUATION OF SAR-SDNLM FILTER FOR CHANGE DETECTION CLASSIFICATION

Mariane S. Reis, Leonardo Torres, Sidnei J. S. Sant'Anna, Corina C. Freitas, Luciano V. Dutra

Brazilian National Institute for Space Research (INPE) – Image Processing Division (DPI)
São José dos Campos, SP – Brazil

{reis, ljmtorres, sidnei, corina, dutra}@dpi.inpe.br

ABSTRACT

This study evaluates the usage of Stochastic Distances Non-local Means (SDNLM) speckle filter in an image from Brazilian Amazon. The objective is to evaluate whether the noise reduction improves land cover and change classification. Results obtained from filtered images were compared with those obtained from unfiltered images and images filtered using Gamma Map. Results shows that, when using region based Bhattacharyya Minimum Distance Classifier, land cover and change classification using both speckle filters has accuracy values statistically equal. Analyzing the filtered images themselves, SDNLM obtained better results in terms of visual quality and edges preservation.

Index Terms— Change Detection, Land Cover Classification, SAR data, Speckle reduction

1. INTRODUCTION

Remote sensing data has been the basis of land use and land cover change studies, because of its synoptic vision of the area of interest, repetitively acquisition and digital format [1]. Although remote sensing community has been more devoted to optic sensors [2], this data has some restrictions regarding the occurrence of rains, clouds, fog and smoke, besides been affected by solar intensity, what can lead to misclassification and, in case of change studies, the detection of false changes or no change at all [3].

Synthetic Aperture Radar (SAR) systems are capable of acquiring image almost independently from these atmospheric conditions, with high spatial resolution [3]. These images has been considered in studies of land cover classification and change detection, mainly in Brazilian Amazon's areas, where the constant cloud covers inhibits the acquisition of adequate optical images along the year.

The speckle phenomenon in SAR images hinders the interpretation of these data and reduces the accuracy of segmentation, classification and analysis of objects contained within the image [4]. Therefore, reducing the noise effect is an important task for SAR analysis, and the multiplicative model is usually used for this purpose. In this paper we

compare Stochastic Distances Nonlocal Means (SDNLM) speckle filter to a well-known filter in literature, by the analysis of filtered and unfiltered images. Images were evaluated by speckle reduction, land cover classification and change classification in a forested area in Brazilian Amazon.

The paper is organized as follows: Section 2 presents the algorithm used to obtain the filtered versions. Section 3 describes used data, area of interest and methods for analysis. Some preliminary results and considerations are discussed in Section 4. Conclusions are presented in Section 5.

2. SAR SPECKLE FILTER

SAR imagery filtering techniques are based on different signal processing strategies. Generally, these strategies consider the multiplicative model and the scattering properties of SAR data.

SDNLM filter was proposed by [5] as improvement of previous work [6]. This filter is based on multiplicative model. SDNLM filter's approach consists in checking which regions can be considered as coming from the same distribution (detection problem) which produced the data which comprises the central block. Information Theory based statistical tests are performed in order to analyse the divergence between two samples. Sets which are not rejected by statistical tests are weighted and used to compute a local mean.

The filter setup can be freely specified by the user, but in this investigation we used the neighborhoods of the central pixel and of its surrounding pixels with the same size of 3×3 pixels and filtering window with 5×5 pixels. Figure 1 illustrates the central patch with center pixel z_1 and its 24 neighboring patches, where the pixels whose center are z_i , $i = 2, \dots, 25$. The restored image in z_1 is a weighted sum of the observations at z_2, \dots, z_{25} , being each weight a function of the p -value ($p(1, i)$) observed in the statistical test of same distribution between two Gamma distributions [5]:

$$w(1, i) = \begin{cases} 1 & \text{if } p(1, i) \geq \eta, \\ \frac{2}{\eta}p(1, i) - 1 & \text{if } \frac{\eta}{2} < p(1, i) < \eta, \\ 0 & \text{otherwise,} \end{cases} \quad (1)$$

in which η is the significance level is determined by the user.

Funded by CNPq grants #307666/2011-5, Capes and FAPESP agencies.

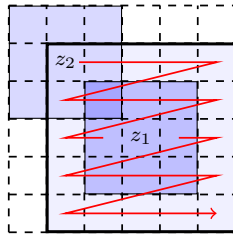


Fig. 1. Central pixel z_1 and its neighboring z_i , $i = \{2, \dots, 25\}$ with 3×3 pixels patches.

3. METHODS

The area of interest in this study is part of the National Forest of Tapajós and its surroundings, located in Belterra, Pará state, in Brazilian Amazon. The region presents humid tropical climate, with mean annual precipitation about 1880 mm and the highest precipitations occurring between January and May. Dominant vegetation is Humid Tropical Rainforest and the terrain has flat surface constitution with portions slightly uneven [7]. The occupation process in region occurred along the BR-163 highway, after the deforestation of primary forest and the opening of roads to establish small farms [7]. As a result of this process, there are mosaics of secondary vegetation in varying stages of development, pasture, croplands and bare soil areas within the forest matrix [8].

Two images from this area were used, one acquired in June, 15th 2008 and the other in June, 21th 2010. These images were acquired by Phase Array L-Band Synthetic Aperture Radar (PALSAR), from Advanced Land Observing System (ALOS) satellite, using Fine Beam Dual (FBD) 1.1 mode. Both images were previously geometric corrected, in order to be co-registered in the same projection and reference system (UTM WGS84, zone 21S). Data was used in intensity format for filtering and amplitude format for classification, in two polarizations (HH and HV), Estimated Number of Looks (ENL) equal to 5 and pixel size 15×15 m.

Each image was filtered using SDNLM, with filtering window = 5×5 ; patches = 3×3 and confidence level = 90%. For comparison, original images were also filtered using Gamma Map filter [9], as implemented in ENVI 4.8, using size window = 5×5 . That said, three images for each date were utilized for analyses: two unfiltered images, referred as PALSAR 2008/2010 and four filtered images referred as PALSAR_Gamma 2008/2010 or PALSAR_SDNLM 2008/2010, depending of the filter utilized.

These images were evaluated in three steps. The first one was to evaluate the images themselves, using the Blind/Referenceless Image Spatial Quality Evaluator (BRISQUE), proposed by [10], which is a holistic measure of quality on no-reference images. It has a score typically between 0 and 100, where 0 represents the best quality and 100 the worst. This image quality evaluator quantifies possible losses of “naturalness” in the image and does not compute distortions. The second analysis was made after a region based classifi-

cation of each image. This classification was made utilizing segmentations from SegSAR [11] for original image and Idrisi’s watershed based segment for filtered images. Five land cover classes were classified. These classes were mature forest (F), secondary vegetation (SV), pasture (PA), cultivated areas (CA) and bare soil (BS). Each image was classified 100 times, using 1200 pixels randomly chosen for each cover class in Bhattacharyya minimum distance classifier [12]. The assigned class for determined region in image is the one most observed among classifications. The kappa index κ of each classification was calculated using a Monte Carlo approach, in which κ was calculated from a confusion matrix constructed from 400 pixels random selected from test samples for each class. This procedure was repeated 10,000 times, and only the mean kappa is presented. Training and test samples were collected from different areas of the image. Kappa values were compared with a Hypothesis Test with 99% of confidence. In the third approach, the resulting classifications were combined using image cross tabulation and reclassified for change classes. Change classes are: No Change (NC), regeneration or abandonment (RA), conversion to pasture (cPA), conversion to agriculture (cAG), Agricultural Cycle (AgCicle), Conversion to Soil (cS) and Deforestation (Dt). Since some transitions are possible when comparing the classifications, but impossible in terrain, these are considered in this work as Impossible Changes (IC). Also, some small rivers (W) were not automatic classified (not enough samples for training), so they were masked to avoid the interference in change analysis. Changes that involve W are referred as Natural Dynamics or Registration Error (DNE). The transitions that result in each class are defined in Table 1 Changes for which it was not encountered test samples (cS, NDE and obviously, IC) were masked. Overall Accuracy (OA) was calculated for the remainder areas of each change classification, using the same approach as κ in step 2. Since IC are clearly errors of classification and the area of unobserved changes in terrain are relatively small, it was considered that the OA of the whole area is approximately the product of OA of unmasked area with the percentage of unmasked area. These resulting change classifications were analyzed considering the probability of occurrence of encountered changes and estimated OA.

Table 1. Change matrix for possible transitions of 2008 and 2010 land cover classifications.

		2010						
		F	SV	PA	BS	CA	W	
2008	F	NC	RA	cPA	Dt	cAG	NDE	
	SV	RA	NC	cPA	Dt	cAG	NDE	
	PA	IC	RA	NC	cS	cAG	NDE	
	BS	IC	RA	cPA	NC	AgCicle	NDE	
	CA	IC	RA	cPA	AgCicle	NC	NDE	
	W	NDE	NDE	NDE	NDE	NDE	NC	

Legend

	Improbable Changes		Impossible Changes
	Probable Changes		No Change

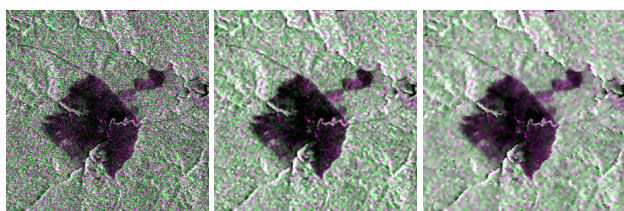
4. RESULTS

Table 2 presents the BRISQUE index, as an form of assessment of the filters in the two intensity channels. The BRISQUE index is better after applying the SDNLM filter in all intensity channels.

Table 2. BRISQUE index applied on PALSAR images and its filtered versions.

	2008		2010	
	<i>HH</i>	<i>HV</i>	<i>HH</i>	<i>HV</i>
PALSAR	67.80	60.33	61.69	61.79
SDNLM	58.43	59.48	59.09	58.62
Gamma	68.94	61.59	61.54	59.41

A subset of the PALSAR 2008 image, 300×300 pixels, is shown in Figure 2(a), as an exemple for visual analysis. The two filters employ a kernel of 5×5 pixels, and the patches in proposal by [5] are 3×3 windows. Figure 2(c) shows the effect of the Gamma Map filter in said subset. Albeit the noise reduction is evident in PALSAR_Gamma, it is also clear that this process introduces some blurring. This blurring eliminates useful information as, for instance, the edges of pasture/forested areas and linear and thin features, in this example rivers and roads. PALSAR_Gamma also presents some saturation among very bright or very dark pixels. The result of the SDNLM filter with $\eta = 90\%$ is shown in Figure 2(b). It is possible to observe that fine details are preserved in this image, while speckle has been reduced. Also, saturation is minimal, when comparing PALSAR_SDNLM with PALSAR_Gamma.

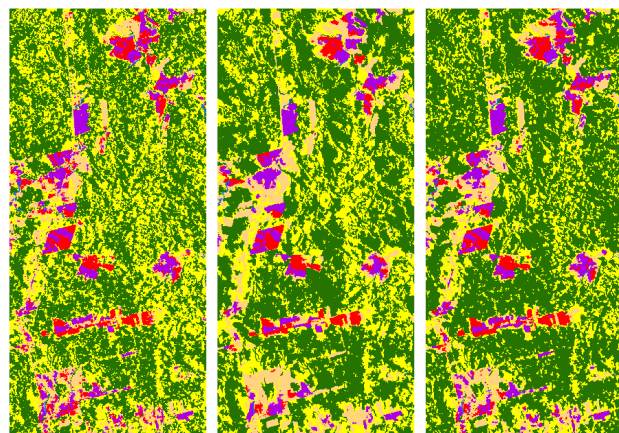


(a) PALSAR (b) PALSAR_SDNLM (c) PALSAR_Gamma

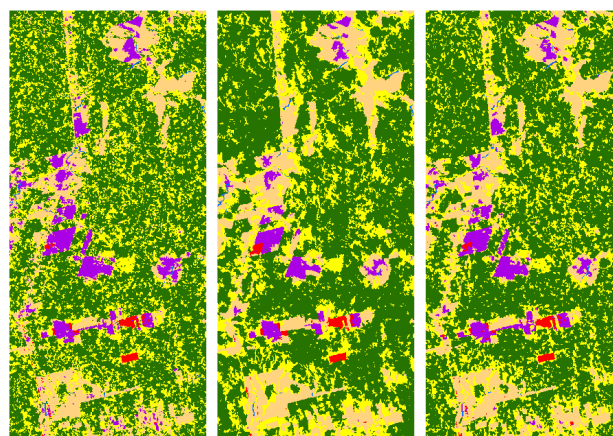
Fig. 2. A subset of 2008 image, in amplitude. Color composition HH (R), HV (G) and HH (B).

Land cover classifications for PALSAR, PALSAR_SDNLM and PALSAR_Gamma for 2008 and 2010 are presented in Figure 3, with respective mean κ . Hypothesis test showed that, for 99% of confidence, κ of filtered images are higher than κ of the unfiltered one for 2010, but equal for 2008. κ calculated for PALSAR_SDNLM and PALSAR_Gamma are equal for both dates.

Figure 4 shows the percentage of classified change classes for each data, grouped by the probability of occurrence. It is possible to observe that PALSAR_SDNLM has the lowest percentage of Impossible Changes, although the dif-



(a) PALSAR 2008, $\kappa = 0.460$ (b) PALSAR_SDNLM 2008, $\kappa = 0.480$ (c) PALSAR_Gamma 2008, $\kappa = 0.486$



(d) PALSAR 2010, $\kappa = 0.547$ (e) PALSAR_SDNLM 2010, $\kappa = 0.626$ (f) PALSAR_Gamma 2010, $\kappa = 0.656$

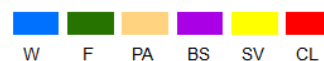


Fig. 3. Land cover classifications obtained from PALSAR image and its filtered versions.

ference between this value and PALSAR_Gamma is very small. PALSAR_Gamma has the lowest value of Improbable Changes, and so the higher value of Probable Changes plus No Change (that is also formed by probable transitions). Considering only this analysis and that classification among the probable change classes and no change in each data are accurate, PALSAR_Gamma achieved better results than PALSAR_SDNLM, and both filtered data were better than the unfiltered one.

Change classifications are presented in Figure 5, along with respective estimated OA. Hypothesis test showed that, considering 99% of confidence, all mean estimated OA are equal. These results reveal that the confusion among transitions that result in NC or probable changes are greater filtered images.

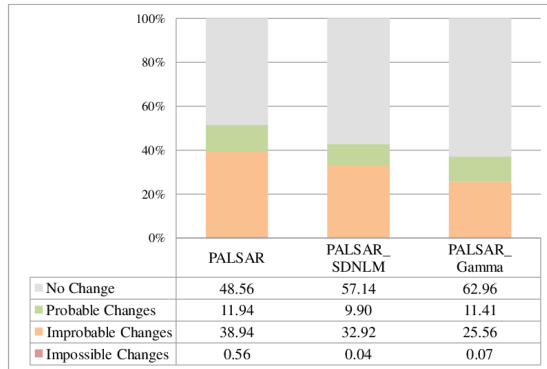


Fig. 4. Percentage of classified change classes for each data, grouped by the probability of occurrence.

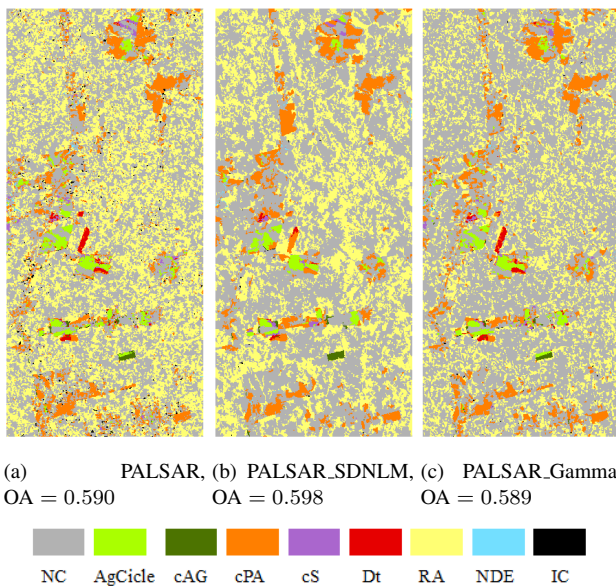


Fig. 5. Land use and land cover change classifications, obtained from PALSAR image and its filtered versions.

5. CONCLUSIONS

When analysing the filtered images themselves, SDNLN filter presented better results than Gamma Map. Besides a better value of BRISQUE for all intensity channels, the usage of this filters improves visual interpretation and allows the identification of thin and small features in the images. For land cover classification, accuracy results were equal between filtered images, and better than unfiltered ones, for both dates. For land cover change classifications, all results were equal.

6. REFERENCES

[1] D. Lu, P. Mausel, E. Brondízio, and E. Moran, “Change detection techniques,” *International Journal of Remote Sensing*, vol. 25, no. 12, pp. 2365–2401, 2004.

[2] L. Bruzzone and F. Bovolo, *Unsupervised change detection in multi-temporal SAR images in Image Processing for Remote Sensing*, CRC Press, Boca Raton, US, 2008.

[3] J.-S. Lee and E. Pottier, *Polarimetric Radar Imaging: From Basics to Applications*, CRC Pres, Boca Raton, US, 2009.

[4] L. Torres, S.J.S. Sant’Anna, C.C. Freitas, and A.C. Frery, “Speckle reduction in polarimetric SAR imagery with stochastic distances and nonlocal means,” *Pattern Recognition*, vol. 47, no. 1, pp. 141–157, 2014.

[5] L. Torres and A.C. Frery, “SAR image despeckling algorithms using stochastic distances and nonlocal means,” in *Workshop of Thesis and Dissertations in SIBGRAPI*, A. Falcão and F. Paulovich, Eds., Arequipa, Peru, 2013, pp. 1–6.

[6] L. Torres, T. Cavalcante, and A.C. Frery, “Speckle reduction using stochastic distances,” in *Pattern Recognition, Image Analysis, Computer Vision, and Applications*, L. Alvarez et al., Ed., Buenos Aires, 2012, vol. 7441 of *Lecture Notes in Computer Science*, pp. 632–639, Springer.

[7] Brazil, “Floresta nacional do Tapajós: Plano de manejo,” Report, volume i (in portuguese), Brazilian Institute of Environment and Renewable Natural Resources (IBAMA), 2004.

[8] M. Escada, S. Amaral, C.D. Rennó, and T.F. Pinheiro, “Levantamento do uso e cobertura da terra e da rede de infraestrutura no distrito florestal da BR-163,” Report (in portuguese), Instituto Nacional de Pesquisas Espaciais (INPE), 2009.

[9] A. Lôpes, E. Nezry, R. Touzi, and H. Laur, “Structure detection and statistical adaptive speckle filtering in SAR images,” *International Journal of Remote Sensing*, vol. 14, no. 9, pp. 1735–1758, 1993.

[10] A. Mittal, A.K. Moorthy, and A.C. Bovik, “No-reference image quality assessment in the spatial domain,” *IEEE Transactions on Image Processing*, vol. 21, no. 12, pp. 4695–4708, 2012.

[11] M.A. Sousa Jr., “Multi-levels and multi-models segmentations for radar and optical images,” Doctoral thesis (in portuguese), Instituto Nacional de Pesquisas Espaciais, São José dos Campos, Brazil, 2005.

[12] R.G. Negri, L.V. Dutra, and S.J.S. Sant’Anna, “Stochastic approaches of minimum distance method for region based classification,” *Progress in Pattern Recognition, Image Analysis, Computer Vision, and Applications Lecture Notes in Computer Science*, vol. 7441, pp. 797–804, 2012.